Cellular uptake and biological activity of peptide nucleic acids conjugated with peptides with and without cell-penetrating ability

Yvonne Turner,[a] Gerd Wallukat,[b] Pille Säälik,[c] Burkhard Wiesner,[a] Stephan Pritz[a] and Johannes Oehlke[a]*

A 12-mer peptide nucleic acid (PNA) directed against the nociceptin/orphanin FQ receptor mRNA was disulfide bridged with various peptides without and with cell-penetrating features. The cellular uptake and the antisense activity of these conjugates were assessed in parallel. Quantitation of the internalized PNA was performed by using an approach based on capillary electrophoresis with laser-induced fluorescence detection (CE-LIF). This approach enabled a selective assessment of the PNA moiety liberated from the conjugate in the reducing intracellular environment, thus avoiding bias of the results by surface adsorption. The biological activity of the conjugates was studied by an assay based on the downregulation of the nociceptin/orphanin FQ receptor in neonatal rat cardiomyocytes (CM). Comparable cellular uptake was found for all conjugates and for the naked PNA, irrespective of the cell-penetrating properties of the peptide components. All conjugates exhibited a comparable biological activity in the 100 nM range. The naked PNA also exhibited extensive antisense activity, which, however, proved about five times lower than that of the conjugates. The found results suggest cellular uptake and the bioactivity of PNA-peptide conjugates to be not primarily related to the cell-penetrating ability of their peptide components. Likewise from these results it can be inferred that the superior bioactivity of the PNA-peptide conjugates in comparison with that of naked PNA rely on as yet unknown factors rather than on higher membrane permeability. Several hints point to the resistance against cellular export and the aggregation propensity combined with the endocytosis rate to be candidates for such factors. Copyright © 2009 European Peptide Society and John Wiley & Sons, Ltd.

Keywords: PNA; cellular uptake; PNA-peptide conjugates; cell-penetrating peptides

Introduction

The value of peptide nucleic acids (PNAs) as a unique class of potent and metabolically stable RNA- and DNA-binding ligands [1] is limited by poor biological activity after administration to living cells [2]. Improved biological activity has been reported repeatedly for PNA chimeras with various peptides [3] ranging from simple cationic sequences [4,5] to protein derived [6–9] and synthetic [9–11] cell-penetrating peptides (CPPs). The benefits of the PNA-peptide conjugates are discussed to be caused by a peptide-mediated facilitation of the delivery into cytosol and nucleus and by an enhanced affinity to the target structures [4,5,12]. The structural requirements for their delivery activity remain unclear so far.

In order to contribute to a better understanding of the effects of tagged peptides on both the intracellular delivery and the bioactivity of PNA, in the present study we have studied the cellular uptake and the antisense activity of various disulfide bridged PNA-peptide chimeras in parallel. To avoid the bias of the uptake data caused by surface adsorption and environmentally influenced fluorescence intensities we used a quantitation approach based on capillary electrophoresis with laser-induced fluorescence detection (CE-LIF). The antisense activity was assessed at a physiological target level by means of a functional assay based on the downregulation of the nociceptin/orphanin FQ receptor in primary heart cells [13,14].

We found comparable internalized quantities for the naked PNA and for the various PNA-peptide conjugates, irrespective of the cell-penetrating properties of their peptide components. In line with the uptake results we found comparable biological activity for the various peptide conjugates but, in distinction, about fivefold lower one for the naked PNA. Our findings suggest the bioactivity of PNA-derivatives to be related to as yet uncharacterized factors rather than to their membrane penetration ability.

* Correspondence to: Johannes Oehlke, Institute of Molecular Pharmacology, Robert-Rössle-Str. 10, D-13125 Berlin, Germany. E-mail: oehlke@fmp-berlin.de

a Leibniz-Institute of Molecular Pharmacology, Robert-Rössle-Str.10, D-13125 Berlin, Germany

b Max Delbrück Center for Molecular Medicine, Robert- Rössle-Str.10, D-13125 Berlin, Germany

c Institute of Molecular and Cellular Biology, University of Tartu, 51010 Tartu, Estonia

Materials and Methods

General

Chemicals and reagents were purchased from Sigma (Deisenhofen, Germany), Bachem (Heidelberg, Germany) or Applied Biosystems (Darmstadt, Germany) unless specified otherwise. Release of lactate dehydrogenase as a measure for the viability of the cells was assessed by means of a freshly prepared reagent containing 5.6 mg sodium lactate, 4.8 mg nicotinamide adenine dinucleotide (NAD) and 1.7 mg K_2HPO_4. To 1 ml of this reagent a 50 µl sample of the supernatant was added and the increase within 2 min of the absorption at 340 nm was measured.

Synthesis of PNA, Peptides and PNA-peptide Conjugates

PNA and peptides

PNA oligomers were synthesized manually using the t-Boc strategy [15]. The peptide segments of the conjugates were synthesized by the solid phase method using standard Boc chemistry [16]. To introduce the fluorescent label, the deprotected *N*-termini of the PNAs or the peptides were reacted in DMF for 3 days at room temperature with 10 equivalents of 5(6)-carboxyfluorescein-*N*-hydroxysuccinimide ester (FLUOS; Boehringer, Mannheim) or for 1 h with three equivalents of dansyl chloride in the presence of six equivalents of diisopropylethylamine.

Purification was carried out by a semipreparative HPLC on Vydac C18 using a 250×8 mm column. MALDI-MS (Voyager-DE STR BioSpectrometry Workstation MALDI-TOF; Perseptive Biosystems, Inc.) provided the expected $[M + H]^+$ peaks.

PNA activation with dithiodipyridine

To activate the PNA for the synthesis of the conjugates, 500 nM of PNA, *C*-terminally tagged with cysteine, was sonicated in 100 µl formamide for 5 min at 60 °C and thereafter reacted with 1 µM of tris(2-carboxyethyl) phosphine for 10 min at 60 °C with sonication to cleave the disulfide bridged PNA portion. Subsequently 67 µM of 2,2′-dithiodipyridine was added and the reaction mixture was maintained at 60 °C for 2 more hours. Thereafter, 400 µl of 0.25 M triethylammonium acetate, pH 9 containing 6 M urea was added and the mixture was extracted five times with 200 µl each of ethyl acetate.

Conjugate assembly and characterization

For reaction with the cysteine-tagged peptides 60 µl of the so obtained solution of the activated PNA was heated to 80 °C and added to 90 µl of an 80 °C warm solution of 400 nmoles peptide in ethanol/water 5/4 v/v. After maintaining for 60 min at 80 °C in a closed vessel the reaction mixture was loaded onto an 80 °C hot precolumn containing 60 mg of PLRP-S 300 A, 8 µm (Polymer Laboratories Ltd, Waltrop, Germany) preequilibrated with eluents A/B 92/8 (A = 0.01 M triethylammonium acetate, pH 9/formamide 4/1 v/v; B = acetonitrile/water/formamide 3.6/0.4/1 v/v/v). Subsequently, the precolumn was washed with 200 µl of eluent A and connected with the HPLC system. The separation was performed at 80 °C using a PLRP-S 300 A, 8 µm column (150 × 4.6 mm; Polymer Laboratories Ltd, Waltrop, Germany) and gradients of 8–70% B (0–15 min), 70–60% B (15–25 min), and 60–8% B (25–30 min) at a flow rate of 1 ml/min. Detection was at 260 nm with simultaneous fluorescence measurement at 540 nm (dansyl) and 520 nm (fluorescein) after excitation at 340 nm and 488 nm, respectively.

The HPLC-fractions containing the conjugates were indicated by simultaneous absorption at 260 nm and dansyl fluorescence at 540 nm (retention times of the residual PNAs and the KLA-conjugates (Table 1) were around 6, and 18–21 min, respectively, while those of the conjugates with more polar peptides were between 11 and 19 min). The fractions were concentrated *in vacuo* to about 20% and the residual formamide solution was heated for 30 min at 80 °C in order to decompose aggregates formed during the evaporation. The measured UV absorption at 260 nm corresponded to yields in the range of 30–50% whereby yields near the lower limit were found for conjugates with less polar peptide moieties. At maximum 10% of noncovalently bound PNA and peptide resisted the HPLC-purification as detected by CE-LIF and measuring the dansyl fluorescence, respectively, and, therefore, these impurities were tolerated in the uptake experiments.

Cleaving of the disulfide bridge and reappearance of the peak of the naked PNA in the CE-LIF electropherogram supported the structure of the synthesized conjugates. However, disulfide splitting could only be achieved at conjugate concentrations lower than 100 nM, by using a large excess of tris(2-carboxyethyl) phosphine or dithiothreitol and after several hours of reaction at 80 °C. At higher conjugate concentrations the degree of cleavage remained negligible, very likely due to an aggregation of the conjugates. Probably for the same reason, MALDI-MS of the conjugates provided mole peaks only for conjugates of the purine rich PNA-1, exhibiting a lower aggregation tendency, and only in the form of small signals exceeding slightly the background noise. Most abundant in the mass spectra of all conjugates were two groups of peaks appearing at *m/z* 2000–3000 and *m/z* 4000–5500 which corresponded to the *N*-terminal half of the PNA and the *C*-terminal half of the PNA linked to the peptide moiety, respectively. This pattern suggests splitting nearly in the middle of the PNA moiety of the conjugates, very likely due to the fact that the maximum laser intensity was required in each case to even generate peaks. MALDI-MS was performed using a Voyager-DE STR BioSpectrometry Workstation MALDI-TOF mass spectrometer (Perseptive Biosystems, Inc.) and a saturated solution of 2,4,6-trihydroxy-acetophenone in 0.05 M diammonium hydrogen citrate/acetonitrile 1/1 as the matrix (Aldrich-Chemie, Steinheim, Germany). Before measuring, the formamide of the conjugate stock solutions was replaced by 0.01 M TFA/acetonitrile 25/75 by means of a Zip Tip RP C18 standard bed (Millipore, Bedford, MA), resulting in 1–10 µM solutions. If more concentrated sample solutions (above 50 µM) were used, the MS-peaks widely disappeared, further suggesting aggregation to be the reason for the observed problems. [M + H] peaks of the parent peptides and PNAs were easily detectable in impure products containing more than about 10% of unreacted peptide or PNA, but normally not in products obtained according to the above described protocol.

Cell Culture

CHO, HEK and MDCK cells were cultured in 24-well plates (5×10^4 cells/well) or for Confocal Laser Scanning Microscopy (CLSM) on 22×22 mm coverslips (1×10^5) at 37 °C in humidified 5% CO_2 containing air environment in Ham's F-12 (CHO) or DMEM (HEK, MDCK) supplemented with 2 mM glutamine and 10% fetal calf serum (FCS) and were used after 4 days. Hela pLuc705 cells [17] (generously provided by Prof. B. Lebleu, University of Montpellier, France) were cultured analogously in DMEM containing 4.5 g/l of glucose, supplemented with 2 mM glutamine and 1% non-essential amino acids. Neonatal rat cardiomyocytes (CM) were

obtained from ventricles of 1–2 day-old Sprague-Dawley rats and cultured as described earlier [18].

Antisense Treatment and Assessment of the Chronotropic Response

Antisense pretreatment of the heart cells was performed on days 1 and 2 after seeding by administration of the conjugates (0.1 μM) or the naked PNA (0.2 μM). To avoid toxic effects the formamide concentration in the incubation medium was confined to maximum 1%.

The chronotropic response of the spontaneously beating neonatal CM was measured as described earlier [18] on day 4 after seeding, every 5 min after cumulative addition of nociceptin/orphanin FQ (FGGFTGARKSARKLANQ) [19,20] at 37 °C.

Westernblot

Cells were lysed in lysis buffer containing 10 mM K_2HPO_4, 150 mM NaCl, 5 mM EDTA, 5 mM EGTA, 1% Triton X-100 + 0.2% deoxy-cholate complemented with protease inhibitor mix and PMSF. Total protein content of 2 μg was separated on a 10% acryl amide gel and blotted to a polyvinylidene difluoride (PVDF) membrane. After saturation of the non-specific binding sites with 5% non fat dry milk (NFDM) solution in tris-buffered saline (TBS), the membrane was hybridized overnight at 4 °C with a primary rabbit polyclonal antibody raised against the *N*-terminus of the nociceptin receptor (6 μg/ml 2,5% NFDM; BioGenes, Berlin, Germany). After washing 3×5 min with 0.1% Tween 20 in TBS, the membrane was incubated with 1 : 1500 alkaline phosphatase-conjugated anti-rabbit secondary antibody (Vector laboratories, CA) for 1 h at room temperature and the signal was developed with BCIP/NBT.

Assessment of Cellular Uptake by Capillary Electrophoresis with Laser-induced Fluorescence Detection (CE-LIF)

The cells were overlayed with 0.2 ml of pre-warmed (37 °C) DPBSG and a corresponding aliquot of the sonicated PNA stock solution was added followed by several times of gentle shaking. If not indicated otherwise, the incubation solution contained 200 nM of the PNA-derivative and 1% of formamide. After incubation at 37 °C for 60 min, the cells were washed four times with ice-cold PBS and the incubation solution was checked for LDH release. The cell damage indicated by the LDH-activity in the incubation solution normally remained below 5% and experiments with values corresponding to higher than 10% damage were discarded. After washing, the cells were lysed for 2 h at 0 °C with 0.2 ml 0.1% Triton X-100 containing 10 mM/l TFA. The lysate, which contained only negligible amounts of fluorescent PNA derivatives (less than 10% of total cell-associated PNA) was used for protein determination according to the Bradford method [21]. The average protein content of 10^6 cells assayed by this method was 180 μg. The average volume of the cells was determined to be 1.2 pl by means of a Coulter-ZM counter (Coulter Electronics Ltd., Luton, England).

The wells containing attached cell debris and nuclei along with bound or precipitated PNA derivative were extracted by sonication for 5 min at 60 °C with 0.2 ml/well tris/borate buffer (20 mM, pH 7.5) supplemented with 5 M urea, 0.1% SDS and, as an internal standard, 10 nM piperidino-Cy5 (obtained by reaction of equimolar amounts of Cy™5 mono-reactive dye (Amersham Pharmacia Biotech, Little Chalfont, England) and piperidine). The resulting extracts were centrifuged for 3 min at 3000 × g and stored at 0 °C; prior to the CE-LIF analysis, 0.5 μl of a 10 mM solution in formamide of the corresponding unlabelled PNA (to displace the fluorescein labelled PNA from complexes with cellular components [11]) was added to each 50 μl portion of the extracts and the mixtures were sonicated for 5 min at 60 °C.

CE-LIF was performed using a P/ACE MDQ system with a P/ACE MDQ Laser-Induced Fluorescence Detector (Beckman Coulter, Fullerton, CA) and a CZESep 600 neutral coated capillary (31 cm, 50 μM ID; Phenomenex, Aschaffenburg, Germany). As the running buffer, 200 mM tris/borate, pH 7.5 with 5 M urea and 0.1% SDS was used. The cell extracts were injected into the capillary for 5 s at 2 pounds per square inch (PSI) and the separations were performed at 400 V/cm and 25 °C. The peaks of the references appeared after 4.3 min (PNA-1-K), 4.7 min (PNA-1) and 5.1 min (piperidino-Cy5) (the uncharged PNA-1 provided a quantifiable peak only in tris-buffer and, in contrast to the charged PNA-1-K, became undetectable after the replacement of the tris base by triethylamine, suggesting generation of a positively charged moiety of PNA-1 by complexing with tris). Because of their altered fluorescence behavior, conjugates normally did not provide fluorescent peaks under the used conditions, except portions with retained or restored fluorescein fluorescence (see Results and Discussion), which appeared as broad peaks in the range of 12–17 min in analogy to the previously studied amide bound PNA-KLA conjugate [11].

Quantitation was performed by fluorescence measurement simultaneously at 520 nm (fluorescein) and 670 nm (piperidino-Cy5) after excitation at 488 nm and 635 nm using an argon ion and a diode laser, respectively. The peaks were integrated using the P/ACE-system MDQ software (Beckman Coulter, Fullerton, CA), and were normalized to the area of the internal standard (piperidino-Cy5) in order to eliminate irregularities of injection and buffer status. Since the exact volume of the sample injected into the capillary remained unknown, the references used as calibration standards were injected under essentially the same conditions in order to eliminate this factor in the subsequent calculations. The concentrations of the references were determined on the basis of the optical density at 260 nm and proved linearly correlated to the peak areas in the range between the quantitation limits and 1 μM. The quantitation limit (signal-to-noise ratio >3) was about 0.5 pM/ml.

Assessment of Cellular Uptake by Confocal Laser Scanning Microscopy

The CLSM measurements were performed using a LSM 510 invert confocal laser scanning microscope (Carl Zeiss Jena GmbH, Jena, Germany) as described previously [22]. In brief, the fluorescent oligonucleotide derivatives were dissolved in 1 ml pre-warmed (37 °C) Dulbecco's phosphate buffered saline supplemented with 1 g/l D-glucose (DPBSG) or DMEM and the cells were overlayed with this solution for 2 h at 37 °C. Subsequent to the observation, the viability of the cells was assessed by the addition of Trypan blue. Excitation was performed at 488 nm (Fluos) and 543 nm (Trypan blue) and emission was measured at 515 nm and 570 nm, respectively. Three regions of interest (ROI's, 16 × 16 pixel; 30 scans with a scan time of 2 s with double averaging) in the cytosol and one in the nucleus of three selected cells were chosen such that the intensity of the diffuse fluorescence could be recorded without substantial interference from vesicular fluorescence. The intracellular fluorescence signal was corrected for the contribution of the extracellular fluorescence, arising from nonideal confocal properties of the CLSM, by estimating the distribution function of sensitivity in the *z* direction of the microscope.

Table 1. Sequence and structural properties of the components of the PNA-peptide conjugates

Compound	Sequence	Structural properties
	Fluos-PNA-Cys-NH$_2$	
	I	
	Dansyl-G-Cys-peptide-NH$_2$	
PNA-1 [11]	Fluos-GGA GCA GGA AAG-Cys-NH$_2$	
PNA-1-K [11]	Fluos-GGA GCA GGA AAG-Lys-NH$_2$	
PNA-2	Fluos-AGG AGC AGG GAA-Lys-NH$_2$	
PNA-3	Fluos-ACC TCA GTT ACA-Cys-NH$_2$	
PNA-4 [17,24]	Ooo-CCT CTT ACC TCA GTT ACA-ooo*	
KLA	Dansyl-G-C-KLALK LALKA LKAAL KLA-NH$_2$	α-helical, amphipathic
KAL	Dansyl-G-C-KALKL KAALA LLAKL KLA-NH$_2$	α-helical, nonamphipathic
KGL	Dansyl-G-C-KGLKL KGGLG LLGKL KLG-NH$_2$	unstructured
ELA	Dansyl-G-C-ELALE LALEA LEAAL ELA-NH$_2$	α-helical, amphipathic
RLA	Dansyl-G-C-RLALR LALRA LRAAL RLA-NH$_2$	α-helical, amphipathic
Pen (Penetratin, [25])	Dansyl-G-C-RQIKI WFQNR RMKWK K-NH$_2$	poor α-helical amphipathic
Tat (Tat 46–57 [26])	Dansyl-G-C-GRKKR RQRRR-NH$_2$	unstructured
VT5 [27]	Dansyl-G-C-DPKGDPKGVTVTVTVTVTGKGDPKPG-NH$_2$	β-sheet, amphipathic

* 2-(aminoethoxy)ethoxyacetic acid spacer.

Results and Discussion

PNA-peptide Conjugates Containing a Fluorescein Label and a Disulfide Bridge Side by Side Exhibit a Pronounced Aggregation Propensity and an Irregular Fluorescence Behavior

In order to get insights into the structural requirements for peptides to deliver PNA into mammalian cells, we have assessed the cellular uptake and the biological activity of disulfidebridged conjugates of a 12-mer PNA complementary to bases 12–23 of the translated region of the nociceptin/orphanin FQ receptor mRNA [13,14]. The peptide components of the conjugates showed systematically altered structure forming properties, charge and size (Table 1). The cellular uptake was assessed by means of a protocol based on capillary electrophoresis with laser-induced fluorescence detection (CE-LIF) [23], which, in distinction to CLSM and FACS, can provide absolute quantities at the femtomole level. Likewise, this protocol enables selective quantitation of the PNA liberated from the disulfide bridged PNA-peptide conjugates in the intracellular reducing environment, thus avoiding bias of the results by surface adsorption.

Unexpectedly the conjugates containing both the fluorescein label and the disulfide bridge, as required for the used protocol, exhibited, other than analogous PNA-peptide constructs bearing only one of these structural elements, an extensive peak broadening under acidic HPLC-conditions and an irregular fluorescence behavior.

As compared with the parent PNA, the conjugates showed significantly weaker intensities in the fluorescence excitation and emission spectra (Figure 1(A) and (B); note the different concentrations used for the spectra of naked PNA and conjugates). Moreover, an aberrant fluorescence behavior of the formed associates is suggested by the increase of the emission, maximum at around 420 nm, accompanying the impairment of the fluorescein-like emission at 520 nm (Figure 1(B)). The dansyl residue of the peptide components has been be ruled out to be responsible for these effects by the similar behavior found of an analogous conjugate lacking this additional label (Figure 1).

The fluorescence behavior of the conjugates could be transformed to that of the naked parent PNA by heating in 8 M
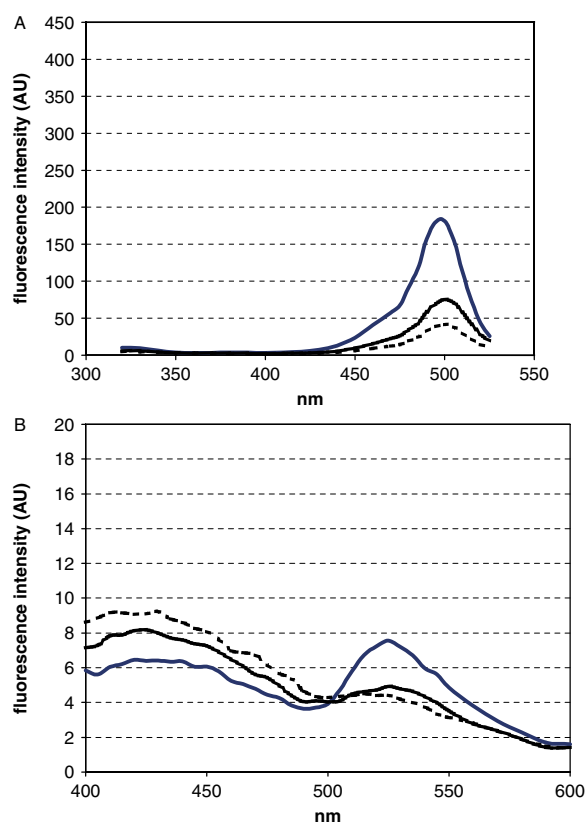

Figure 1. Flurescence spectra of PNA and PNA-peptide conjugates. Fluorescence-excitation- (with emission at 540 nm; **A**) and – emission spectra (after excitation at 340 nm; **B**) in PBS of PNA-1 (100 nM) (———) and PNA 1, disulfide bridged with KLA (- - - -) and KLA devoid of the dansyl label (grey) (each 800 nM).

urea/ethanol 2/1 or formamide at 80 °C for at least 30 min (not shown), suggesting that self-association was responsible for the observed deviations. An unchanged UV intensity at 260 nm before

and after such treatment and a lack of precipitation indicated the formed associates to be completely soluble.

Both, the conjugates showing the aberrant and the restored fluorescein-like fluorescence status, provided identical cellular uptake results (data not shown), suggesting that the associate formation is not relevant for the cell penetration. This notion is supported also by the comparable biological activities of the disulfide bridged KLA-conjugate of PNA-1 and its regularly behaving amide linked analog (see below).

On the other hand, the irregular fluorescence behavior of these conjugates prevented more detailed studies including also the quantification and the compartmentalization of the cell-associated intact conjugates. Moreover, if interpreted as a more general phenomenon, such aberrant fluorescence behavior might give rise to principal errors in fluorescence-based protocols like CLSM or FACS, being not adequately considered so far.

The PNA-peptide Conjugates were Extensively Taken Up by Mammalian Cells Irrespective of the Structural Properties of their Peptide Components

The measured quantities of the naked PNA liberated by intracellular disulfide splitting corresponded in all cases to intracellular concentrations approaching the conjugate concentrations in the external incubation solutions (related to a ratio of about 7 µl cell volume/mg protein, see Materials and Methods) (Figure 2). The cellular uptake proved to be linearly dependent on the external concentration in the range of 0.1–1 µM (Figure 3). The uptake differences between PNA conjugates with peptides of structural properties like positive charge, amphipathicity and reduced polarity, which are thought to be common characteristics of CPPs [28], and peptides lacking such features, remained within one order of magnitude (Figure 2, Table 1), from which it can be inferred that these features play only a minor role in the membrane penetration of the conjugates.

However, it is worth noting that the assessed PNA quantities represent only a lower limit of the uptake, because only the split and not the intact portions of the internalized conjugates could be detected by the used CE-LIF protocol. The upper limit
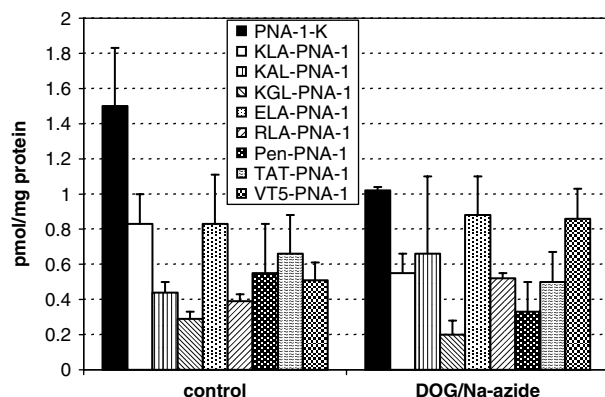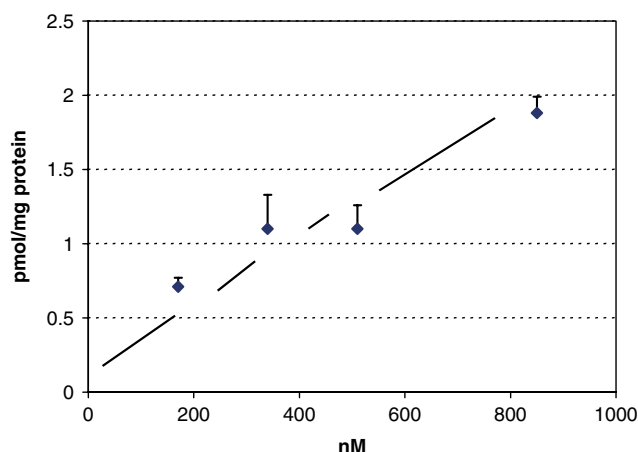
Figure 3. Quantities of intracellular PNA measured after exposing cells to different concentrations PNA conjugated with KLA. Quantities of intracellular PNA-1 measured by CE-LIF after 60 min exposure at 37 °C of HEK cells to different concentrations of the conjugate of PNA-1 with KLA dissolved in DPBS (the intercept at the y-axis is caused by memory effects of the capillary). Each bar represents the mean of three samples ± SEM. This figure is available in colour online at www.interscience.wiley.com/journal/jpepsci.

of the uptake can be derived from the results obtained in a previous study performed with the amide-linked PNA-KLA analog [11]. In this study we found intracellular concentrations for the intact conjugate corresponding to about fivefold of the external concentration, but we were unable to rule out the possibility that this value was overestimated due to the surface adsorption of the conjugate.

PNA-peptide Conjugates Internalize into Cells Partially Through Non-endocytotic Mechanisms

Energy depletion caused small decrease, if any, in the internalization of the conjugates (Figure 2), indicating that the uptake proceeds primarily in a non-endocytotic way. The internalization of several of the conjugates was even enhanced after deoxyglucose/NaN$_3$ treatment (Figure 2), suggesting the involvement of structure- and energy dependent export processes counteracting the uptake under normal conditions.

Moreover, in contrast to the widespread belief that naked PNAs are unable to enter cells non-endocytotically, we found that naked PNAs internalized similarly to the PNA-peptide conjugates (Figure 2). Although, in the case of the naked PNA, some ambiguity caused by surface adsorption cannot be ruled out, the respective bias of the uptake results should remain below 20% according to our previous investigations [11]. The bioactivity of the naked PNA found in our previous work [11] and in this study (see below) also ensures the cellular uptake of PNA itself.

The uptake of both naked PNAs and conjugates by non-endocytotic modes became increasingly impaired during their storage in physiological buffer, very likely due to the formation of associates which are unable to cross the plasmamembrane. This behavior is illustrated by the drastic drop of the cellular internalization of conjugates (by 85% for PNA-1-KLA and 50% for PNA-1-Pen as well as the naked PNAs PNA-1 and PNA-1-K; data not shown) which was observed if the incubation solutions were stored in physiological buffer for 60 min at 37 °C before addition to the cells.
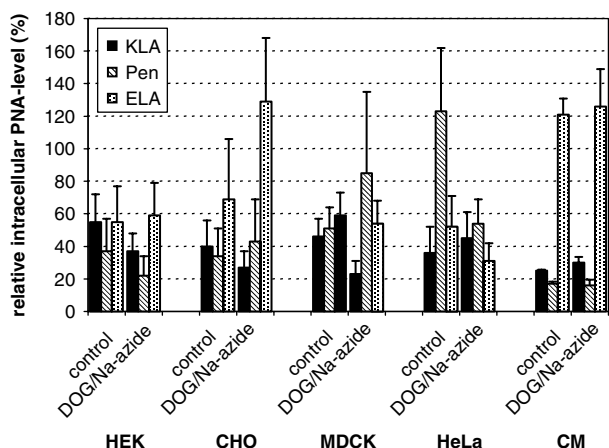
Figure 2. Quantities of intracellular PNA measured after exposing HEK cells to PNA-peptide conjugates without and with energy depletion. Quantities of intracellular PNA-1 and PNA-1-K measured by CE-LIF after 60 min exposure at 37 °C of HEK cells to 200 nM solutions in DPBSG or DPBS containing 25 mM 2-deoxyglucose/10 mM sodium azide, respectively, of conjugates of PNA-1 with various peptides and of PNA-1-K. Before addition of the conjugates the cells were preincubated in DPBSG or DPBS containing 25 mM 2-deoxyglucose/10 mM sodium azide, respectively, for 60 min at 37 °C. Each bar represents the mean of at least six samples ± SEM.

Figure 4. Quantities of intracellular PNA measured after exposing various cell types to PNA-peptide conjugates without and with energy depletion. Relative quantities of intracellular PNA-1 measured by CE-LIF after 60 min exposure at 37 °C of various cells to 200 nM solutions in DPBSG or DPBS containing 25 mM 2-deoxyglucose/10 mM sodium azide, respectively, of conjugates of PNA-1 with various peptides. Before addition of the conjugates the cells were preincubated in DPBSG or DPBS containing 25 mM 2-deoxyglucose/10 mv sodium azide, respectively, for 60 min at 37 °C. The quantities of PNA-1 were normalized as percentages of the internalized quantities of PNA-1-K measured in the respective experiment after incubation with 200 nM PNA-1-K in DPBSG as a standard. Each bar represents the mean of three samples ± SEM.

Figure 5. CLSM image of a 1-μm-thick central horizontal optical section through HEK cells pre-exposed for 120 min at 37 °C to 1 μM solutions in DPBSG of PNA-1-KLA. The image shows an overlay of the fluorescence (Ex/Em 488 nm/515 nm) and the transmission micrographs.

The Cellular Uptake of PNA-peptide Conjugates Exhibits Cell Type Dependence

Examination of the internalization of the conjugates into various cell types revealed significant differences under both normal conditions and energy depletion (Figure 4). These differences were dependent on the peptide structure and cell type, indicating the existence of various possible non-endocytotic transport mechanisms in mammalian cells. Likewise, this variability appears promising as a basis for approaching cell or tissue selective delivery with PNA-peptide conjugates.

Assessment of the Cellular Uptake of Various PNA-peptide Conjugates and Naked PNAs by CLSM Revealed Significant Diffuse Cytosolic Fluorescence

Investigations of cells exposed to the various PNA-peptide chimeras and naked PNAs with CLSM revealed comparable diffuse fluorescence in cytosol and nucleus accompanied by some punctuate cytosolic fluorescence in all cases (as a typical example, cells exposed to PNA-1-KLA are displayed in Figure 5). These findings indicate endocytotic as well as non-endocytotic uptake for all conjugates and naked PNAs. The measured fluorescence intensities remain in accordance with the CE-LIF results within one order of magnitude (Figure 6) and suggest also the cell-penetrating ability of PNA-peptide conjugates to be not primarily dependent on the cell-penetrating features of the tagged peptides.

In contrary to the CE-LIF results, the PNA conjugated with KLA, which includes both amphipathic properties and basic side chains (Table 1), resulted in higher intracellular fluorescence compared to the other conjugates (Figure 6). This discrepancy might be seen in conjunction with the different conditions used in both protocols (culturing at a lowered cell density and exposing the cells to a higher substrate concentration in the case of CLSM and a consequently higher sensitivity to the membrane perturbing
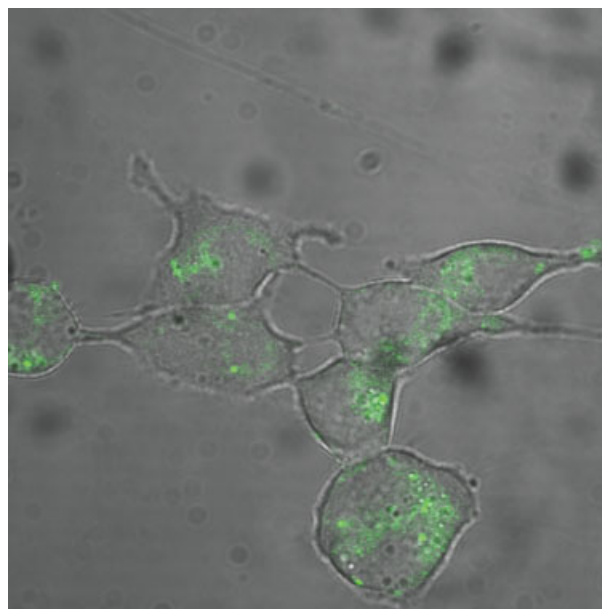
activity of the KLA-sequence). It might refer, also, to possible synergistic effects of the structural features of the KLA-sequence, resulting in better cellular uptake. Furthermore, one can look at this discrepancy as a possible enhancement of the endocytotic uptake of this conjugate due to a higher aggregation propensity (see below). Generally, however, the reliability of the fluorescence intensities measured by CLSM is clearly lower than that of the quantities assessed by the CE-LIF protocol so that the observed CLSM values should be taken less seriously than the CE-LIF results.

PNA Conjugates with Peptides Bearing Cell-penetrating Structural Elements Exhibited Comparable Antisense Activity to Conjugates Lacking these Properties

To obtain information about the influence of the tagged peptide moieties on the biological activity of PNA, we have assessed the antisense activity of the conjugates in the same way as described previously for the analogous amide-linked PNA-KLA [11]. Principally, the assay is based on influencing the positive chronotropic effect on the beating rate of spontaneously beating neonatal rat CM exerted by the neuropeptide nociceptin [19,20]. The PNA component served as a sequence complementary to bases 12–23 of the translated region of the nociceptin/orphanin FQ receptor mRNA [13,14] (PNA-1, Table 1). Benefits of this protocol consist of the physiological target level and the cytosolic location of the target.

In line with the uptake results, we found comparable antinociceptin activity around the 100 nM level for all investigated conjugates (Figures 7 and 8). Conjugates bearing peptides with structural elements regarded to be characteristic of CPPs, such as positive charges or amphipathicity [28], exhibited only moderately stronger antisense effects compared to those containing peptides without secondary structure forming properties (PNA-1-KGL) or even bearing negative charge (PNA-1-ELA (Figures 7 and 8, Table 1). In contrast to the uptake results, which had revealed comparable uptake levels for both naked PNA and conjugates,
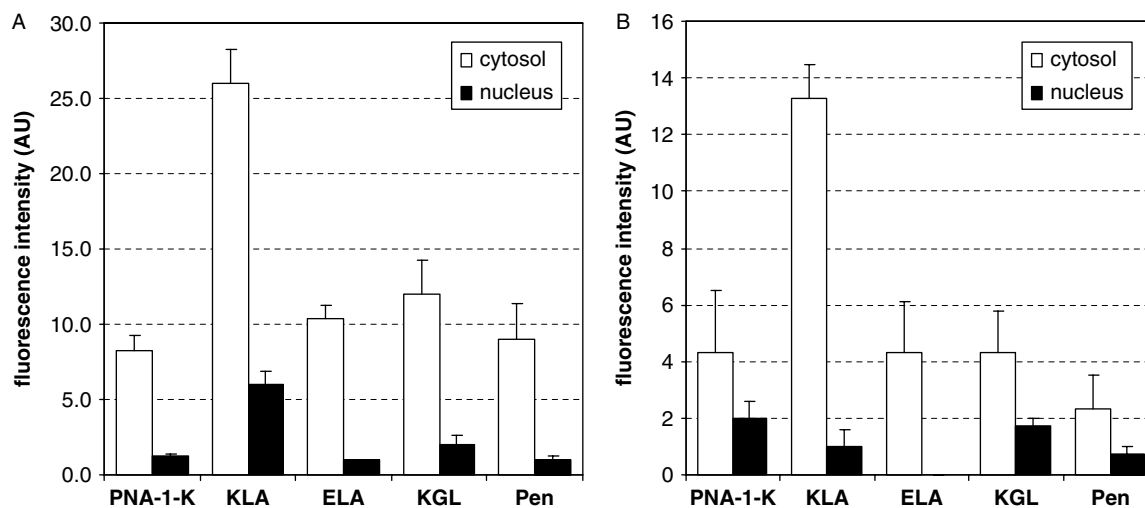
Figure 6. Intracellular fluorescence intensities after exposing cells to various PNA-peptide conjugates and naked PNA. Fluorescence intensity in cytosol and nucleus of HEK cells (A) and HeLa pLuc705 cells (B) measured by CLSM after incubation with 1 µM solutions in DPBSG of PNA-1-K and conjugates of PNA-1 with various peptides for 120 min at 37 °C. The fluorescence intensities were normalized by subtracting the corresponding background fluorescence intensities of untreated cells. Each bar represents the mean of three cells ± SEM.
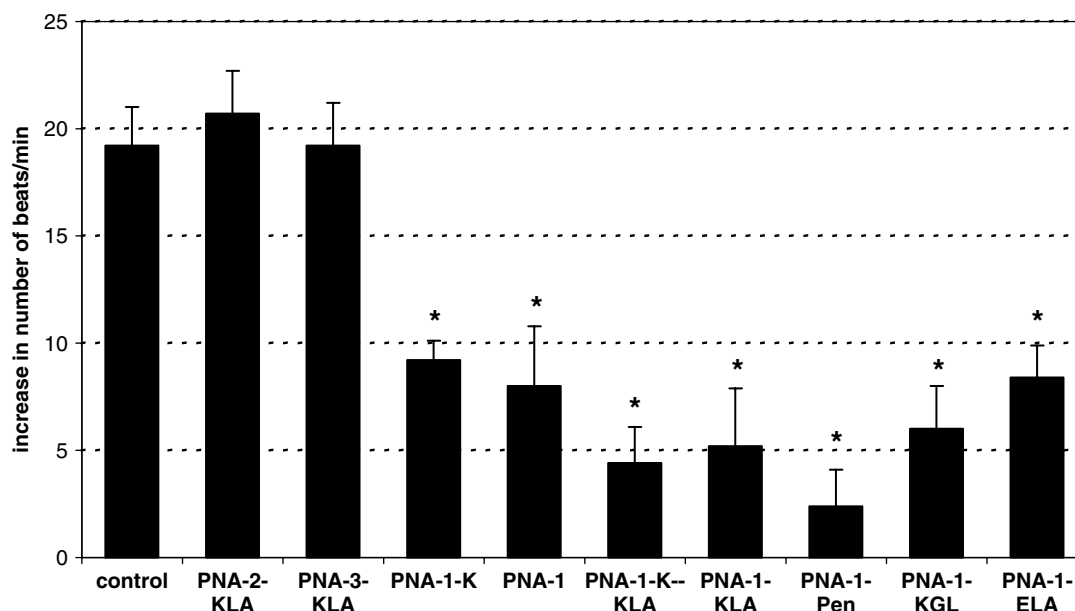

Figure 7. Antisense activity of PNA-peptide conjugates and naked PNA. Influence of 10^{-5} M nociceptin on the beating rate of spontaneously beating neonatal CM measured on day 4 of culture without and with pretreatment with 0.1 µM of various peptide-chimeras of PNA-1 or 0.2 µM of PNA-1, PNA-1-K, PNA-2-KLA and PNA-3-KLA on day 1 and 2 after seeding. The basal beating rate of the CM on day 4 of culture was 148 ± 6 beats/min (SD; $n = 8$). Each bar represents the mean of 8 cells or cell cluster ± SEM. The difference between the control and the asterisk-marked bars are statistically significant at $P \leq 0.05$ (Student's t-test).

we found, however, an about two to five times lower antisense activity for the naked PNA as compared to that of the conjugates (Figures 7 and 8).

Virtually identical antinociceptin activity was found for both the amide-bound PNA-1-K-KLA conjugate and its disulfide bridged analog PNA-1-KLA (Figure 7) suggesting the bioreversibility of the PNA-peptide linkage to be of minimal importance for the biological activity and the preceding uptake step.

The pretreatment of CM with the conjugates revealed no influence on their basal beating rate, indicating that the PNA derivatives are nontoxic at the used concentration. KLA conjugates with a scrambled and an unrelated 12-mer PNA (PNA-2, PNA-3, Table 1) did not show any antinociceptive effect (Figure 7), implicating that the anticipated antisense downregulation of the nociceptin receptor was the mechanism of the biological effect of PNA-1. This notion was further supported by the *western blot* analysis of the nociceptin receptor protein in CM pretreated with PNA-1-KLA or the inactive control PNA-3-KLA (Figure 9). Detection with the antibody directed against the *N*-terminus of the nociceptin receptor revealed a strong smear band at 55 kDa in control cells, corresponding to the molecular size of the nociceptin receptor. However, in good agreement with results from bioactivity experiments, the band was not detected in lysates of cells pretreated with the antisense conjugate (Figure 9).
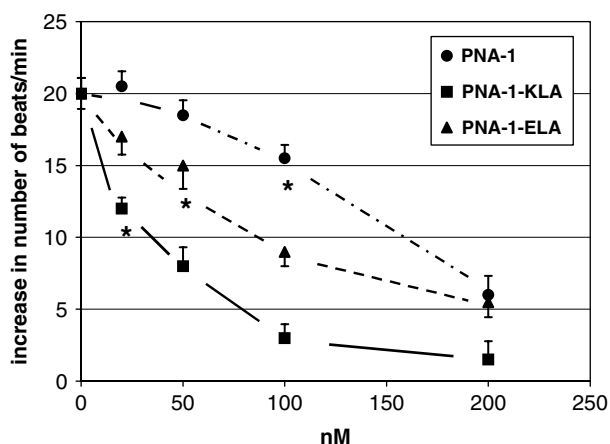
Figure 8. Concentration dependence of the antisense activity of PNA-peptide conjugates and naked PNA. Influence of 10^{-5} M nociceptin on the beating rate of spontaneously beating neonatal CM measured on day 4 of culture after pretreatment with different concentrations of PNA-1, PNA-1-KLA or PNA-1-ELA on day 1 and 2 after seeding. Each point represents the mean of 8 cells or cell cluster ± standard error of the mean (SEM). The differences between the control (0 nM PNA) and the asterisk-marked points (as well as those belonging to the respective higher PNA concentrations) are statistically significant at $P \leq 0.05$ (Student's *t*-test). The same applies to the mutual differences between the PNA-derivatives at 100 nM pretreatment.
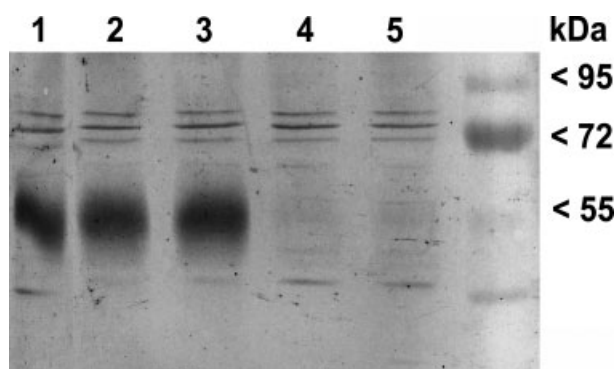

Figure 9. Western analysis of the downregulation of the nociceptin receptor in neonatal CM. Western analysis of the nociceptin receptor expression in the lysates of untreated neonatal rat CM (lane 1) and after pretreatment with 0.1 µM PNA-3-KLA (unrelated; lanes 2, 3) or 0.1 µM PNA-1-KLA (antisense; lanes 4, 5).

As Yet Uncharacterized Factors Influence the Bioactivity of PNA-peptide Conjugates to At Least the Same Extent as the Membrane Permeability

Seen in this context, from our findings it can be inferred that the cell-penetrating properties of the tagged peptides are not mandatory for the ability of PNA to enter cells and to exert antisense activity. Likewise, the comparable uptake levels but distinct antisense activities found for naked PNAs and conjugates, respectively, suggest alternative, as yet unknown factors to have at least the same importance for the biological activity of PNA-derivatives as the membrane permeability. About the nature of such factors can only be speculated at the present state.

Enhanced affinity to the target [29] seems unlikely to play a considerable role in our case, if the large structural diversity of the used peptide moieties and the nevertheless comparable activity of the various conjugates are considered.

More likely different affinities of naked PNA and conjugates to energy dependent cellular export machineries might belong to such factors. Hints in this direction are provided by the effects of energy depletion observed here (Figures 2 and 4) and previously [11] and the significantly lower re-export found previously for the internalized amide-bound KLA-PNA as compared to that of the naked PNA [11].

As a further factor, the different propensity to form associates of conjugates and naked PNA could play a role in this context. In contrast to the here performed uptake experiments, the endocytotic uptake of the formed associates might become relevant in functional assays which, as in the present case, mostly
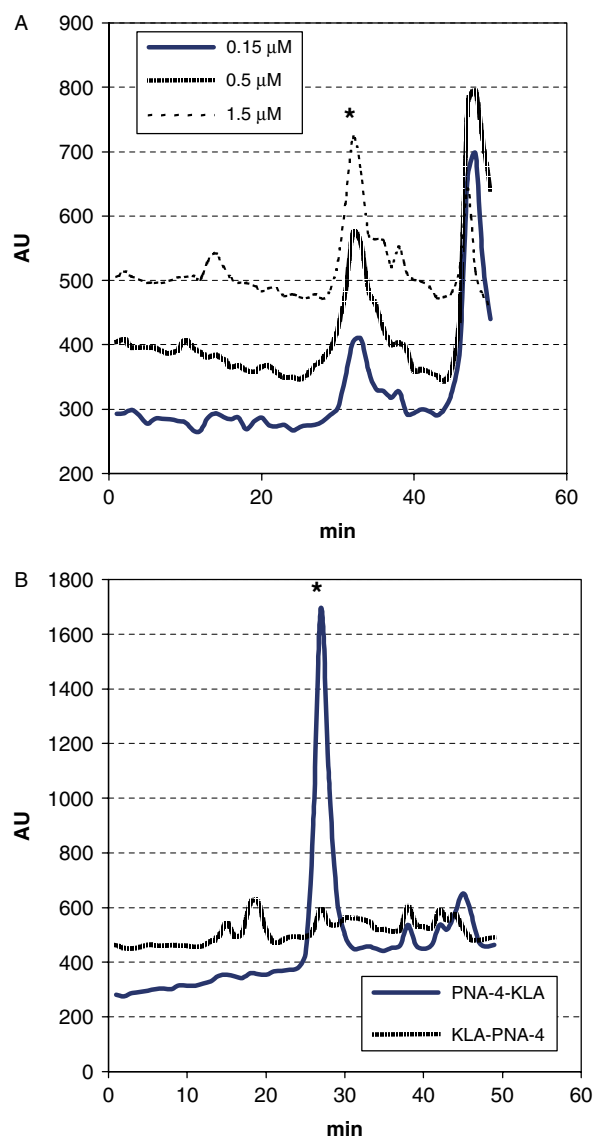

Figure 10. Size exclusion chromatography investigation of the aggregation propensity of various PNA-peptide conjugates. Size exclusion chromatograms after loading each 50 µl of 0.15 µM, 0.5 µM and 1.5 µM PNA-1-KLA (A) or 0.2 µM PNA-4-KLA and KLA-PNA-4 (B) freshly dissolved in PBS onto a Superdex 75 HR 10/30 column (Pharmacia Biotech). The elution was performed with 10 mM phosphate buffer, pH 7.4 containing 150 mM NaCl and 20% acetonitrile at a flow rate of 0.5 ml/min and detection at 260 nm. (* The asterisk labeled peaks correspond to the monomeric form and later appearing peaks correspond to, due to adsorption to the sephadex support, irregularly behaving entities).

need much longer incubation periods. The high tendency to form associates of the conjugates used here, is illustrated by size exclusion chromatograms showing an apparent concentration independence of the monomer peak (chromatograms of PNA-1-KLA performed at different concentrations as representatives are shown in Figure 10(A)). This behavior refers to the formation of particles which are unable to pass through the chromatography column, already at the medium nanomolar range. The naked PNA, on the other hand, was found preferentially in the monomeric form even at 2 μM concentration (not shown).

Support for such relation between bioactivity and aggregation propensity is provided by size exclusion chromatograms of conjugates used in a previous splicing correction study [24]. These conjugates contained also the peptide moieties listed in Table 1 and, additionally, aggregation inhibiting polyethylenglycol spacers [24]. In most cases they exhibited only moderate splicing correction activities. As exceptions, however, the KLA-construct (KLA-PNA-4, Table 1) and its RLA analog exhibited more than two orders of magnitude higher splicing correction activities for reasons which remained unclear at that time [24]. Size exclusion chromatography studies now revealed these highly active derivatives to exist in physiological buffer almost exclusively in the form of aggregates being unable to pass through the chromatography column already at 150 nM concentration (Figure 10(B)). In contrast, the moderately active conjugates remained in physiological buffer in the monomeric form even at 2 μM concentration (as a representative the chromatogram of PNA-4-KLA, Table 1, is shown in Figure 10(B)). Addition of the lysosomotropic reagent chloroquine, further enhanced the bioactivity of the highly aggregated conjugates but, let nearly unaffected the monomeric ones [24], suggesting endocytosis to be involved in the former case. In this context, these findings suggest the splicing correction activity of these conjugates to be strongly related to both their aggregation propensity and the extent of their internalization by endocytotic modes.

Benefits of an endocytotic delivery in comparison to that of a non-endocytotic one could consist of the circumvention of export mechanisms counteracting a non-endocytotic uptake and, additionally, in the formation of intracellular depots enabling a steady release of PNA. In light of the ability of PNA found here and in other studies to cross biomembranes non-endocytotically [11,30–32,] the escape from the endocytotic vesicles, commonly regarded to be the main drawback of an endocytotic internalization, should not pose serious problems. Moreover, the repeatedly reported but widely neglected ability of common oligonucleotides to penetrate mammalian plasma membranes non-endocytotically [33–37,] lets such interpretation to also appear valid for their cationic lipid-mediated delivery.

Conclusions

In conclusion our study revealed comparable cellular uptake for various PNA-peptide conjugates and for naked PNAs. The uptake differences between conjugates bearing CPP-resembling peptides and such others which are unstructured and even negatively charged remained within one order of magnitude. Correspondingly, comparable antisense activity was measured for the various conjugates but, in contrast to the uptake results, an about five times lower one was seen for the naked PNA. These findings suggest that the biological activity of PNA derivatives is not primarily related to their ability to penetrate biomembranes.

Several hints point to the aggregation propensity combined with the endocytosis rate to be an alternative factor affecting noticeably the bioavailability of PNA-peptide conjugates.

References

1 Zanta MA, Belguise Valladier P, Behr JP. Gene delivery: a single nuclear localization signal peptide is sufficient to carry DNA to the cell nucleus. *Proc. Natl. Acad. Sci. U. S. A.* 1999; **96**: 91–96.

2 Pooga M, Land T, Bartfai T, Langel U. PNA oligomers as tools for specific modulation of gene expression. *Biomol. Eng.* 2001; **17**: 183–192.

3 Gait MJ. Peptide-mediated cellular delivery of antisense oligonucleotides and their analogues. *Cell. Mol. Life Sci.* 2003; **60**: 844–853.

4 Kaihatsu K, Braasch DA, Cansizoglu A, Corey DR. Enhanced strand invasion by peptide nucleic acid-peptide conjugates. *Biochemistry* 2002; **41**: 11118–11125.

5 Kaihatsu K, Huffman KE, Corey DR. Intracellular uptake and inhibition of gene expression by PNAs and PNA-peptide conjugates. *Biochemistry* 2004; **43**: 14340–14347.

6 Basu S, Wickstrom E. Synthesis and characterization of a peptide nucleic acid conjugated to a D-peptide analog of insulin-like growth factor 1 for increased cellular uptake. *Bioconjugate Chem.* 1997; **8**: 481–488.

7 Simmons CG, Pitts AE, Mayfield LD, Shay JW, Corey DR. Synthesis and membrane permeability of PNA-peptide conjugates. *Bioorg. Med. Chem. Lett.* 1997; **7**: 3001–3006.

8 Koppelhus U, Awasthi SK, Zachar V, Holst HU, Ebbesen P, Nielsen PE. Cell-dependent differential cellular uptake of PNA, peptides, and PNA-peptide conjugates. *Antisense Nucleic Acid Drug Dev.* 2002; **12**: 51–63.

9 Turner JJ, Ivanova GD, Verbeure B, Williams D, Arzumanov AA, Abes S, Lebleu B, Gait MJ. Cell-penetrating peptide conjugates of peptide nucleic acids (PNA) as inhibitors of HIV-1 Tat-dependent trans-activation in cells. *Nucleic Acids Res.* 2005; **33**: 6837–6849.

10 Pooga M, Soomets U, Hallbrink M, Valkna A, Saar K, Rezaei K, Kahl U, Hao JX, Xu XJ, Wiesenfeld Hallin Z, Hokfelt T, Bartfai A, Langel U. Cell penetrating PNA constructs regulate galanin receptor levels and modify pain transmission in vivo. *Nat. Biotechnol.* 1998; **16**: 857–861.

11 Oehlke J, Wallukat G, Wolf Y, Ehrlich A, Wiesner B, Berger H, Bienert M. Enhancement of intracellular concentration and biological activity of PNA after conjugation with a cell-penetrating synthetic model peptide. *Eur. J. Biochem.* 2004; **271**: 3043–3049.

12 Astriab-Fisher A, Sergueev D, Fisher M, Shaw BR, Juliano RL. Conjugates of antisense oligonucleotides with the Tat and antennapedia cell-penetrating peptides: Effects on cellular uptake, binding to target sequences, and biologic actions. *Pharm. Res.* 2002; **19**: 744–754.

13 Tian JH, Xu W, Zhang W, Fang Y, Grisel JE, Mogil JS, Grandy DK, Han JS. Involvement of endogenous orphanin FQ in electroacupuncture-induced analgesia. *Neuroreport* 1997; **8**: 497–500.

14 Zhu CB, Cao XD, Xu SF, Wu GC. Orphanin FQ potentiates formalin-induced pain behavior and antagonizes morphine analgesia in rats. *Neurosci. Lett.* 1997; **235**: 37–40.

15 Christensen L, Fitzpatrick R, Gildea B, Petersen KH, Hansen HF, Koch T, Egholm M, Buchardt O, Nielsen PE, Coull J. Solid-phase synthesis of peptide nucleic acids. *J. Pept. Sci.* 1995; **1**: 175–183.

16 Stewart JM, Young JD. *Solid Phase Peptide Synthesis*. Pierce Chemical Comp., Rockford: Illinois, 1984.

17 Kang SH, Cho MJ, Kole R. Up-regulation of luciferase gene expression with antisense oligonucleotides: Implications and applications in functional assay developments. *Biochemistry* 1998; **37**: 6235–6239.

18 Wallukat G, Nemecz G, Farkas T, Kuehn H, Wollenberger A. Modulation of the beta-adrenergic response in cultured rat heart cells. I. Beta-adrenergic supersensitivity is induced by lactate via a phospholipase A2 and 15-lipoxygenase involving pathway. *Mol. Cell. Biochem.* 1991; **102**: 35–47.

19 Meunier JC, Mollereau C, Toll L, Suaudeau C, Moisand C, Alvinerie P, Butour JL, Guillemot JC, Ferrara P, Monsarrat B. Isolation and structure of the endogenous agonist of opioid receptor-like ORL1 receptor. *Nature* 1995; **377**: 532–535.

20 Reinscheid RK, Nothacker HP, Bourson A, Ardati A, Henningsen RA, Bunzow JR, Grandy DK, Langen H, Monsma F-JJ, Civelli O. Orphanin FQ: a neuropeptide that activates an opioidlike G protein-coupled receptor. *Science* 1995; **270**: 792–794.

21 Bradford MM. A rapid and sensitive method for the quantitation of microgram quantities of protein utilizing the principle of protein-dye binding. *Anal. Biochem.* 1976; **72**: 248–254.

22 Lorenz D, Wiesner B, Zipper J, Winkler A, Krause E, Beyermann M, Lindau M, Bienert M. Mechanism of peptide-induced mast cell degranulation – translocation and patch-clamp studies. *J. Gen. Physiol.* 1998; **112**: 577–591.

23 Rosati R, Adil MR, Ali MA, Eliason J, Orosz A, Sebestyen F, Kalemkerian GP. Induction of apoptosis by a short-chain neuropeptide analog in small cell lung cancer. *Peptides* 1998; **19**: 1519–1523.

24 Wolf Y, Pritz S, Abes S, Bienert M, Lebleu B, Oehlke J. Structural requirements for cellular uptake and antisense activity of peptide nucleic acids conjugated with various peptides. *Biochemistry* 2006; **45**: 14944–14954.

25 Derossi D, Joliot AH, Chassaing G, Prochiantz A. The third helix of the Antennapedia homeodomain translocates through biological membranes. *J. Biol. Chem.* 1994; **269**: 10444–10450.

26 Vives E, Brodin P, Lebleu B. A truncated HIV-1 Tat protein basic domain rapidly translocates through the plasma membrane and accumulates in the cell nucleus. *J. Biol. Chem.* 1997; **272**: 16010–16017.

27 Oehlke J, Krause E, Wiesner B, Beyermann M, Bienert M. Extensive cellular-uptake into endothelial cells of an amphipathic beta-sheet forming peptide. *FEBS Lett.* 1997; **415**: 196–199.

28 Langel U (ed.). Cell-Penetrating peptides. *Handbook of Cell-Penetrating Peptides*, 2nd edn. CRC Press LLC: Boca Raton, 2007.

29 Corey DR. 48000-fold acceleration of hybridization by chemically modified oligonucleotides. *J. Am.Chem. Soc.* 1995; **117**: 9373–9374.

30 Tyler BM, McCormick DJ, Hoshall CV, Douglas CL, Jansen K, Lacy BW, Cusack B, Richelson E. Specific gene blockade shows that peptide nucleic acids readily enter neuronal cells *in vivo*. *FEBS Lett.* 1998; **421**: 280–284.

31 Kaihatsu K, Shah RH, Zhao X, Corey DR. Extending recognition by peptide nucleic acids (PNAs): binding to duplex DNA and inhibition of transcription by tail-clamp PNA-Peptide conjugates. *Biochemistry* 2003; **42**: 13996–14003.

32 Good L, Nielsen PE. Antisense inhibition of gene expression in bacteria by PNA targeted to mRNA. *Nat. Biotechnol.* 1998; **16**: 355–358.

33 Marti G, Egan W, Noguchi P, Zon G, Matsukura M, Broder S. Oligodeoxyribonucleotide phosphorothioate fluxes and localization in hematopoietic cells. *Antisense Res. Dev.* 1992; **2**: 27–39.

34 Gao WY, Storm C, Egan W, Cheng YC. Cellular pharmacology of phosphorothioate homooligodeoxynucleotides in human cells. *Mol. Pharmacol.* 1993; **43**: 45–50.

35 Temsamani J, Kubert M, Tang J, Padmapriya A, Agrawal S. Cellular uptake of oligodeoxynucleotide phosphorothioates and their analogs. *Antisense Res. Dev.* 1994; **4**: 35–42.

36 Hartmann G, Krug A, Bidlingmaier M, Hacker U, Eigler A, Albrecht R, Strasburger CJ, Endres S. Spontaneous and cationic lipid-mediated uptake of antisense oligonucleotides in human monocytes and lymphocytes. *J. Pharmacol. Exp. Ther.* 1998; **285**: 920–928.

37 Oehlke J, Birth P, Klauschenz E, Wiesner B, Beyermann M, Oksche A, Bienert M. Cellular uptake of antisense oligonucleotides after complexing or conjugation with cell-penetrating model peptides. *Eur. J. Biochem.* 2002; **269**: 4025–4032.